Multivariable Shape Actuation Capabilities Envelopes of Vertical-Stack Mills

Recent developments in describing shape actuation complexities and capabilities of highly coupled 20-high cluster mills offer an extension of the classical control range roll gap profile/geometry characterization in terms of the rolled transverse stress distribution (shape), spanning high orders of odd and even curvature. This article examines the shape actuation capabilities envelopes of 4-high and 6-high mills, with a focus on their application to mill setup and scheduling.

Author

Mark E. Zipf
formerly, control, automation and drive system technologies, Tenova I2S, Yalesville, Conn., USA
mzipf@istmg.com

This article is the third in a series by Mark E. Zipf. The first part was published in the December 2012 issue, and the second in the February 2013 issue, of *Iron & Steel Technology.*

A framework for describing the shape actuation characteristics of rolling mills involves depicting the extent of a mill's capabilities as a continuous, closed region of a linearly algebraic vector space, whose basis set (orthogonal directions) is formed over the field of ordered transverse spatial curvatures (i.e., first order: slope; second order: parabolic; third order: cubic, etc.). This region is often termed the "control range."[1,2] The chosen basis set (coordinate system) can reflect the geometric components of the roll gap profile[1,2] or the curvatures of the material's transverse stress pattern (shape).[3,4] By evaluating the shape actuators and mill setup over their operating ranges, the collection of spatial curvatures from the resulting profiles or stress patterns can be over-contained by a closed region (or envelope). This region specifically defines the nature and extent of the contribution of spatial curvature orders that can be provided by the shape actuators.[1–4] Figure 1 provides an illustration of a typical 6-high mill and the control ranges of the roll gap profile and spatial curvature coordinate systems.

A common/classical method used in the control range analysis of vertical stack arrangements involves mathematical modeling[1,2] of the transverse roll gap profile/geometry and evaluating it over the operating range of the rolls' mechanical crowns and shape actuation. Here, a 2D space that spans the quadratic curvature and a composite collection of even, higher-order terms of the geometric curvatures serves as the coordinate basis with dimensional units (typically expressed in µm). The resulting control ranges appear as closed, 2D regions (Figure 1).

This straightforward approach provides sound insight for general evaluations and visualizations. Unfortunately, this technique is purely theoretical and its results cannot be directly measured, which compromises model validation. Further, because of its dimensional/gap profile nature, the direct transformation to shape/flatness characterizations can be misleading, especially in assessing shape target reachability.[4]

Recent developments in characterizing the shape actuation capabilities of highly coupled 20-high cluster mills[3,4] offer an extension of the classical control range roll gap profile characterization of vertical stack mill shape actuation by describing the spatial curvatures of the

Figure 1

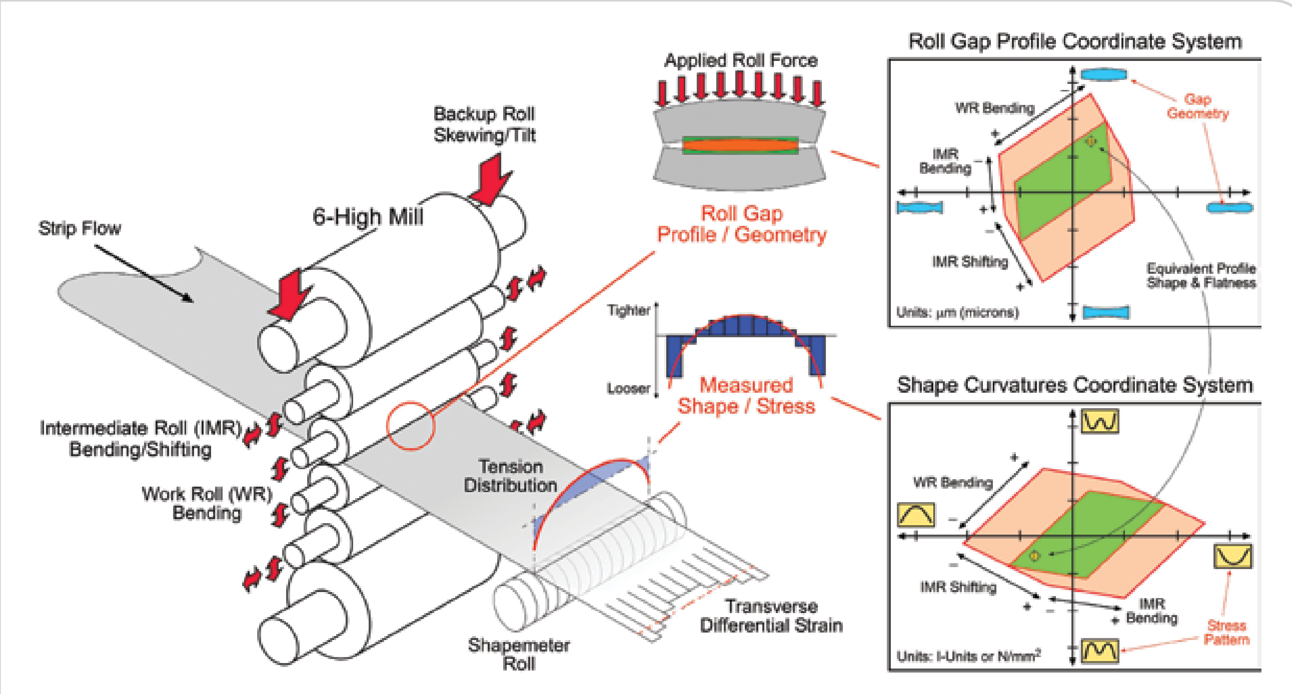

Roll gap profile geometry and stress pattern (shape) curvature coordinate systems applicable to rolling mill shape actuation capabilities modeling.

rolled strip's differential, transverse stress distribution. Here, the spatial influence functions of the mill's multiple shape actuators are described by a fully adapting, computationally efficient matrix model (formed from modeling and empirical studies[5]). The model has sufficient dexterity to be able to accommodate all aspects of the shape actuators' behavior (including roll stack tilting/skewing, roll bending, roll shifting and zonal coolant). The transverse resolution of the model can be arbitrarily selected/adjusted to accurately portray fine scale characteristics, like a single coolant zone response.

The spatial curvature constituents of the actuators' transverse shape/stress waveform patterns are based on orthogonal polynomial representations, which span odd and even orders of curvature, typically up to the eighth order (but can also range to the 60th or higher order to accommodate individual zonal coolant sprays). The orthogonal polynomial representations not only provide a convenient means of describing the spatial curvatures, but inherently form a spatial curvature vector space basis set (coordinate system) that is analytically expedient.

The transformation between the transverse spatial waveforms (stress patterns) and their associated spatial curvatures is based on an orthogonal polynomial decomposition method[6–8] (originating from function approximation theory[9]), which is akin to the relationship between a time response and its corresponding frequency response/Bode diagram. This parameterizing decomposition is based on inner product characteristics of the orthogonal polynomials, which is implemented by linear algebraic matrix methods.

A given arbitrary setting of the shape actuators and the resulting transverse shape/stress waveform pattern are uniquely characterized by a single vector (point) within the orthogonal polynomial vector space. By evaluating the entire range of the constrained actuation settings, it is possible to "map out" the entire set of vectors (points) describing the rolled shape patterns amenable to the actuation system. Through continuity, this set of vectors (spatial curvature constituents of the actuated/rolled shapes) spans a continuous region of the curvature vector space that can be over-contained/bounded by a closed, piecewise continuous curve/surface. This curve can be determined by using image processing edge detection methods[10] to identify the region's extremities and the associated bounding curve segments. This bounding curve and closed region have been termed the shape actuation capabilities envelope (SACE).[3] Figure 2 provides a comparative illustration of the multipass SACEs associated with a 20-high cluster mill and 6-high vertical stack mill.

For a particular condition (strip width, thickness, yield stress, separating force, etc.), the resulting curve/surface forms an envelope that describes the extent of the actuation's shape adjustment capabilities for that

Figure 2

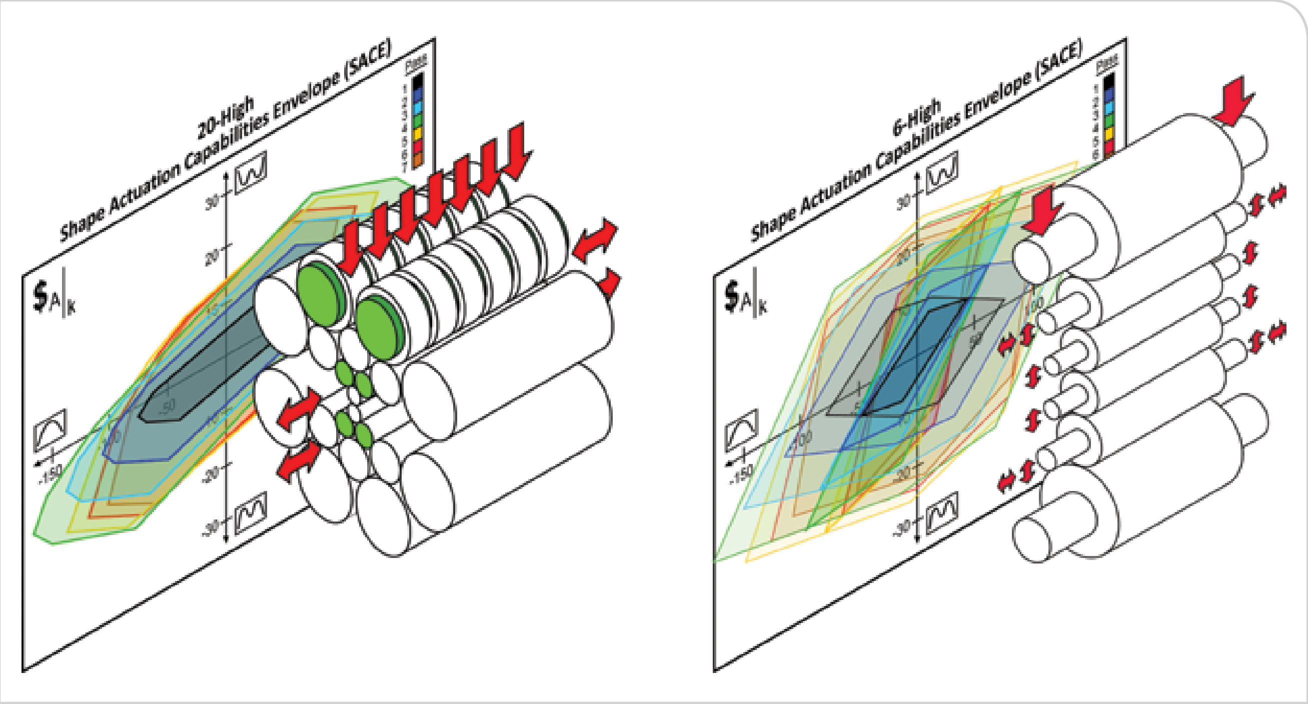

Conceptual illustrations of the multipass SACEs of a 20-high cluster mill (left) and 6-high vertical stack mill (right).

instance and situation. Examining the nature and relationships of these SACEs for a variety of different operating conditions (e.g., over the pass-to-pass progression of thickness and yield stress changes) provides the ability to define the range of available shape actuation corrections for given situations. This provides much-needed insight into the available pass schedules, shape targets and roll stack setups that can be accommodated by the mill.

The key advantages of using this shape/stress-based approach over the classical roll gap profile/geometry method are as follows:

- Based on a consistent analytic framework that is abstracted from and independent of the mill configuration and arrangement.
- Arbitrary transverse spatial resolution (fine enough to accommodate zonal coolant sprays).
- The orthogonal polynomial representations provide spatial curvature descriptions and an inherent vector space basis set (coordinate system).
- Fully scalable odd and even orders of curvature (up to and beyond the 60th order).
- Computationally efficient analytic framework.
- Applicable to asymmetric transverse strip thickness profiles (wedged strip).

And perhaps most importantly:

- The orthogonal polynomial coordinate system is scaled in shape/stress units and is therefore directly applicable to shape target reachability studies.[4]
- The results can be directly measured and validated by on-line shapemeter readings.

Vertical Stack Mill Shape Actuation

Vertical stack 6-high mills adjust the strip's shape (stress pattern) by coordinating a set of actuators to modify the applied transverse pressure distribution, thereby altering the localized strip elongation/strain and resulting transverse stress/tension distribution of the rolled strip. The shape actuation systems on 4-high mill configurations are similar, but form a reduced set of capabilities; therefore, the broader range of the 6-high arrangement will be the point of interest in this discussion. A common actuation configuration[2] is shown in Figure 3.

Static and Dynamic Shape Adjustment Mechanisms — There are several organizations/philosophies associated with the mill setup (diameter profiles of the rolls within the stack, complex crowns, tapers, etc.) and static/dynamic allocations of the shape actuators. However, these are all based on the same underlying mechanical structure. Table 1 provides a listing of

Figure 3

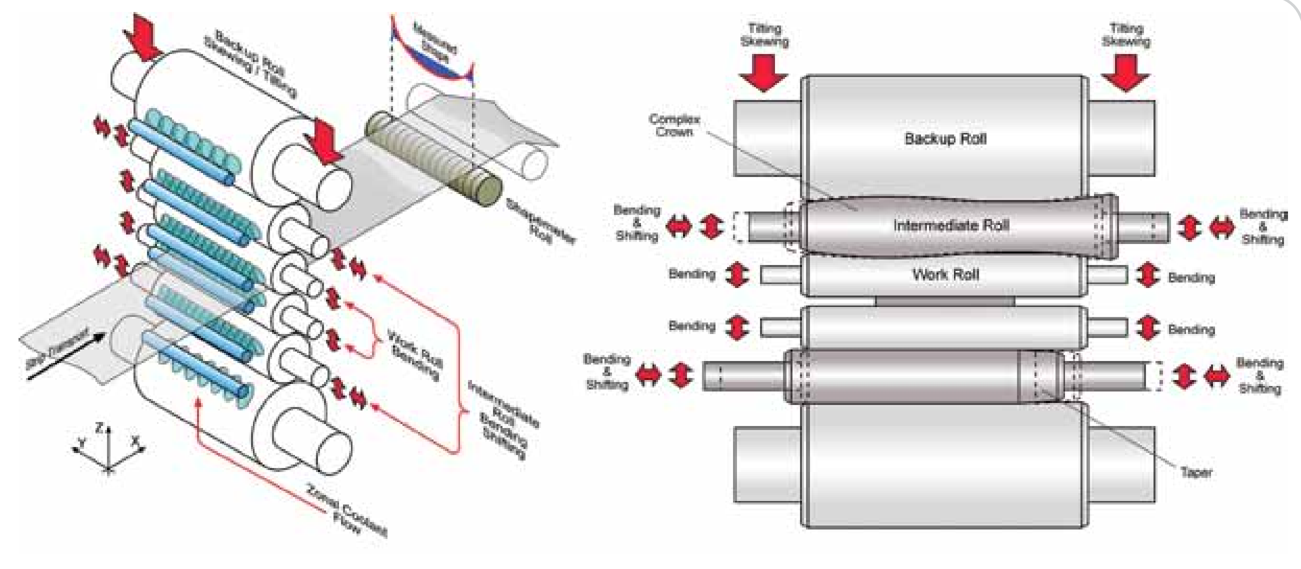

A typical 6-high mill arrangement and shape control actuators.

Table 1

Shape Acuators, Their Static/Dynamic Capabilities and Speed of Response

Shape actuator	Action: Static	Action: Dynamic	Action: Dynamic response
Work rolls (WR)	Mechanical crown Roll bending preset	Roll bending	Fast
Intermediate rolls (IMR)	Complex crowns Tapers	Lateral shifting	Slow
	Lateral shifted preset Roll bending preset	Roll bending	Fast
Backup rolls (BUR)	Mechanical crown Tapers	Skewing/tilting	Fast
Coolant application	Basic sprays	Zonal sprays	Slow

the shape actuators, their static/dynamic actions and speeds of response.

It is important to note the various combinations of static and dynamic shape actuation and their speeds of response. The static actions are associated with the off-line selection of roll diameter crown profiles (mechanical crown) and the presets of shape actuators to best compensate for the expected roll stack deformations, thermal conditions and incoming strip profile. The design of these compensations depends on the material (geometry and work hardening) and intended operating point (i.e., reduction, separating force, speed, etc.). Therefore, the reduction plan/pass schedule is also a component in the static shape actuation.

The dynamic actions are associated with on-line shape correction/control. These actions are partitioned by their actuation speed of response. The fast-acting dynamics are provided by the servo-controlled hydraulic roll force cylinders and roll bending systems (see text in red in Table 1). The rate of lateral shifting of complex crowned intermediate rolls is constrained by the inter-roll surface contact frictions and rolling speed (to provide protection from inducing excessive stress on the coupling and thrust bearing mechanisms). The thermally induced zonal coolant adjustments are the slowest performers, but have the ability to obtain complex patterns (high orders of transverse spatial curvature) of shape compensation.

Shape Actuator Spatial Influence Functions — Each actuator induces a unique transverse stress adjustment pattern/reaction that can be characterized by a continuous spatial influence function (waveform pattern). These spatial influences are not localized to the vicinity of the actuator's physical location, but span the strip width, due to the manner in which the roll stack mechanically reacts/deforms and subsequently distributes the actuator forces to the roll bite. The actuator influence functions are non-linear and have highly coupled interactions that, by definition, have a zero mean so as to be non-interactive with the thickness control system (AGC). As shown in Figure 4, the behavior of these functions varies greatly over the material characteristics, operating conditions and mill setup philosophy.

Figure 4

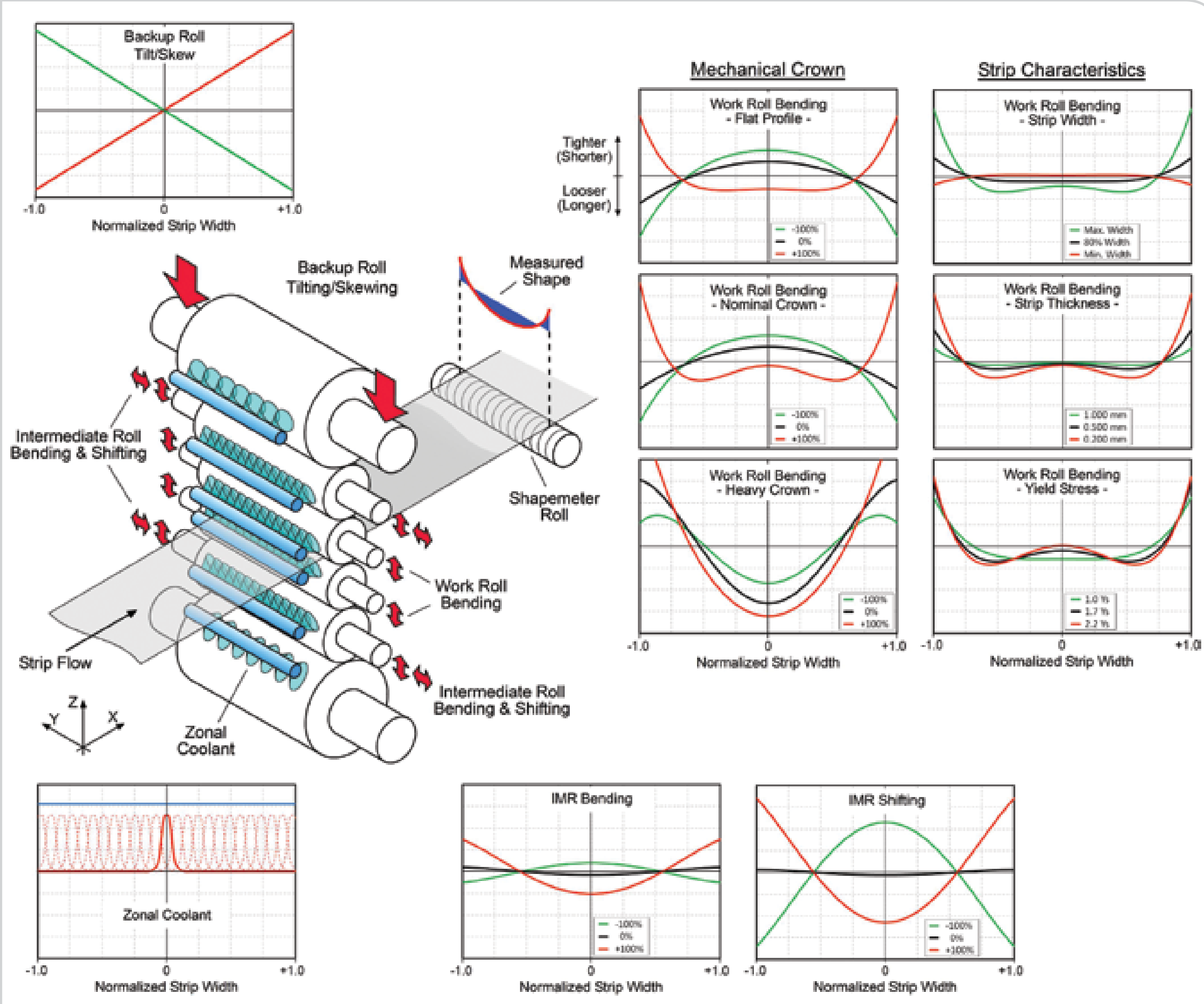

Shape actuation transverse spatial influence functions.

Dynamic Spatial Model — It is possible to describe the transverse stress pattern of the rolled strip by the combined effects of the actuators' influences, the incoming strip stress pattern and the deformation characteristics of the roll stack/mill under separating force load.[3,4,6–8] Based on a discrete spatial model, this vector relationship is shown in Figure 5 and given by:

$$\mathbf{S}_T(y_M) \sim \mathbf{S}(y_M) = \mathbf{S}_0(y_M) + \mathbf{S}_R(y_M) + \mathbf{S}_A(y_M)$$

Discrete Spatial Function

(Eq. 1)

where these components are the discrete, spatial representations of the transverse shape/stress waveform patterns, given by:

$\mathbf{S}(y_M)$ $\triangleq$ Rolled/exiting strip shape vector (stress pattern) produced by the mill, given by:

$$\mathbf{S}(y_M) = \left[S\left(y_M^0\right) \quad S\left(y_M^1\right) \quad \cdots \quad S\left(y_M^{M-1}\right) \right]^T$$

(Eq. 2)

The elements of this vector are the stress amplitudes at the corresponding transverse locations of y_M.

$\mathbf{S}_T(y_M)$ $\triangleq$ Shape target vector, indicating the desired shape of the rolled/exit strip.

$\mathbf{S}_0(y_M)$ $\triangleq$ Incoming strip shape vector. This component is static for the evaluated situation.

$\mathbf{S}_R(y_M)$ ≜ Natural mechanical deformation characteristics of the roll stack and mill while under separating force loading. This component is static and cannot be modified during on-line/rolling operations.

$\mathbf{S}_A(y_M)$ ≜ Shape/stress waveform pattern induced by the shape actuators.

The discrete spatial variable, y_M, is an M-dimensional set of uniformly distributed locations across the strip width, W, which have been mapped to the normalized domain interval [–W/2, +W/2]→[–1, 1] of a Sobolev space.

$$y_M = \left\{ y_M^0, y_M^1, \cdots, y_M^{M-1} \right\} \text{ with the requirement of:}$$

$$y_M^0 = -1 \text{ and } y_M^{M-1} = +1$$

(Eq. 3)

Shape Actuator Model — The dynamic shape actuation contribution, $\mathbf{S}_A(y_M)$, is represented by the matrix multiplication of the N-dimensional shape actuation vector, $\mathbf{A} \in \Re^N$, onto the spatial influence function matrix, $\mathbf{G}_M \in \Re^{MxN}$ (see Equations 4–5, below).[3,4,6–8]

In this linear algebraic framework, the spatial waveform characteristics of the mill's transmission of the shape actuator settings is provided through a matrix, $\mathbf{G}_M$, whose columns are the evaluations of the individual actuator's spatial influence at the sampling grid associated with y_M. It is important to note, depending on the number of applied actuators and the resolution of the y_M sampling grid, $\mathbf{G}_M$ may not be square.

The central relationship of Equation 1 becomes:

$$\mathbf{S}_T(y_M) \sim \mathbf{S}(y_M) = \mathbf{S}_0(y_M) + \mathbf{S}_R(y_M) + \mathbf{G}_M\mathbf{A}$$

(Eq. 6)

A key aspect of Equations 1 and 6 is that $\mathbf{S}_R$ is a static adjustment and $\mathbf{S}_A(\mathbf{G}_M\mathbf{A})$ is a dynamic adjustment. Further, $\mathbf{S}_0$ of the second and subsequent passes is the shape target of the previous pass.

$$\mathbf{S}_0(y_M)\big|_k = \mathbf{S}_T(y_M)\big|_{k-1}$$

k is the pass index: k = 2, 3, 4, …

(Eq. 7)

The actuator spatial influence functions can be derived from analytic modeling[11,12] or through direct on-line evaluation of the mill's response characteristics.[5] This process involves probative measurement of the individual actuator's spatial influence function, and least squares fitting of the measured spatial waveform, to determine the continuous polynomial representation, $Q_i(y)$.[3] Figure 6 provides a block diagram illustration of this process.

The elements of the $\mathbf{G}_M$ column vectors are determined by direct evaluation of the polynomial, $Q_i(y)$, at the specific discrete locations in y_M. This process is continued as the overall product mix is rolled (online) or simulated (off-line), establishing a broad database of responses and identified parameters. Using Monte Carlo-like techniques, this database ultimately provides a sufficiently full population of all operational conditions considered. The evolution of this population allows the details of the spatial influence functions' variations due to material characteristics,

Equations 4–5

$$\mathbf{S}_A(y_M) = \mathbf{G}_M\mathbf{A}$$

(Eq. 4)

where

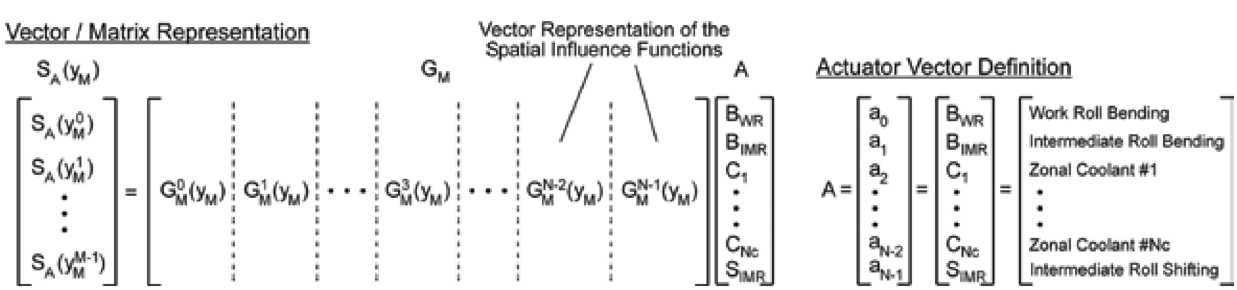

(Eq. 5)

Figure 5

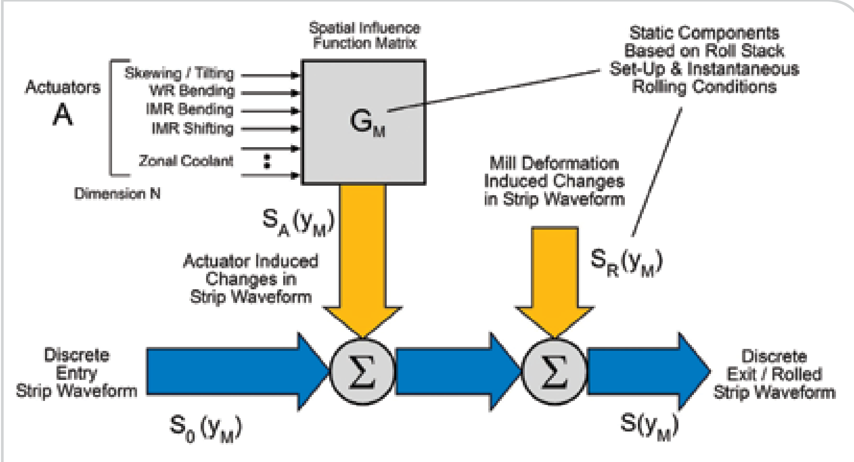

Block diagram model of the transverse contributions of the components that form the rolled/exit strip waveform pattern in a 6-high mill.

operating conditions and mill setup to be examined. This expanding (and overlapping) population also provides a refining quality to the modeled results.

This paper will focus only on the symmetric/even response characteristics, and therefore will not consider the primarily odd/slope contributions of the roll force cylinder skewing/tilting. However, the odd terms are always available for use in situations where the strip profile is asymmetric (slit or wedged strip) and in cases where the incoming stress pattern is asymmetric or diagonal stress is present due to conical or dished coiling behavior.

Roll Stack Deformation — Under separating force loading, the roll stack deformation characteristic, $\mathbf{S}_R(y_M)$, is a function of the roll diameter profiles (mechanical crowns), the lateral positions of the complex crowns or tapers on the IMRs, and the instantaneous rolling conditions (including separating force, rolling speed, strip width, thickness and yield stress). In general, $\mathbf{S}_R(y_M)$ is a static vector composed of primarily of even, second- through eighth-order spatial curvatures.

Available Freedoms in Adjusting the Rolled Strip Shape — Together, the actuated dynamic component, $\mathbf{S}_A(y_M)$, and the static component, $\mathbf{S}_R(y_M)$, constitute the available degrees of freedom in adjusting the rolled strip shape, both actively and as part of a process engineering design (i.e., the selection of the roll stack setup, the actuator presets and tuning of the pass schedule separating forces).

The shape actuation-induced stress patterns, $\mathbf{S}_A(y_M)$, are fundamentally constrained by both physical limitations and operational/protective constraints. These constraints limit the extent of the actuators' ability to dynamically address deviations between the rolled/exit strip shape and the desired shape target, $\mathbf{S}_T(y_M)$, during rolling operations.

The design of $\mathbf{S}_R(y_M)$ is a complex "black art" that involves paying careful attention to the roll stack diameter profiles and pass schedule to program the progression of the mill deformation over the pass-to-pass sequence. The important aspect of this shape adjustment component is that it can be modified only by exchanging rolls within the stack or pass schedule, and not during rolling operations.

Spatial Curvature Characterization Through Parameter Decomposition — The spatial waveform patterns of the strip shape components of Equations 1 and 6 (i.e., $\mathbf{S}_0$, $\mathbf{S}_R$, $\mathbf{S}_A$) can be described by a simplifying vectoral distribution/spectrum of spatial curvatures.[3,4,6–8] An Approximation Theory[9] approach uses an orthogonal polynomial basis (coordinate system) to frame the description of the shape patterns/waveforms. Here, the spatial characteristics of the shape patterns/waveforms are described by the combination of orthogonal polynomial-based spatial curvatures.

Spatial Waveform Approximation Using an Orthogonal Polynomial Basis — In the appropriate Sobolev space, the set of Gram orthogonal polynomials[3,6–8] forms a complete basis set. Therefore, functions occurring in the continuous domain $-1 \le y \le 1$ can be expressed/approximated by the truncated expansion:

$$\mathbf{S}(y) = \sum_{i=1}^{N_p} \mathbf{\$}_S^i \, \mathbf{P}_i(y) \qquad \text{(Eq. 8)}$$

where

$P_i(y) \triangleq$ Gram polynomials.

$\mathbf{\$}_S^i \triangleq$ Coefficients indicating the contribution weighting of the individual polynomials (curvature spectrum).

$N_p \triangleq$ The desired cutoff in the degree/order of curvature used in making the approximation.

This polynomial basis method of approximation describes specific degrees of spatial curvature (in the

Figure 6

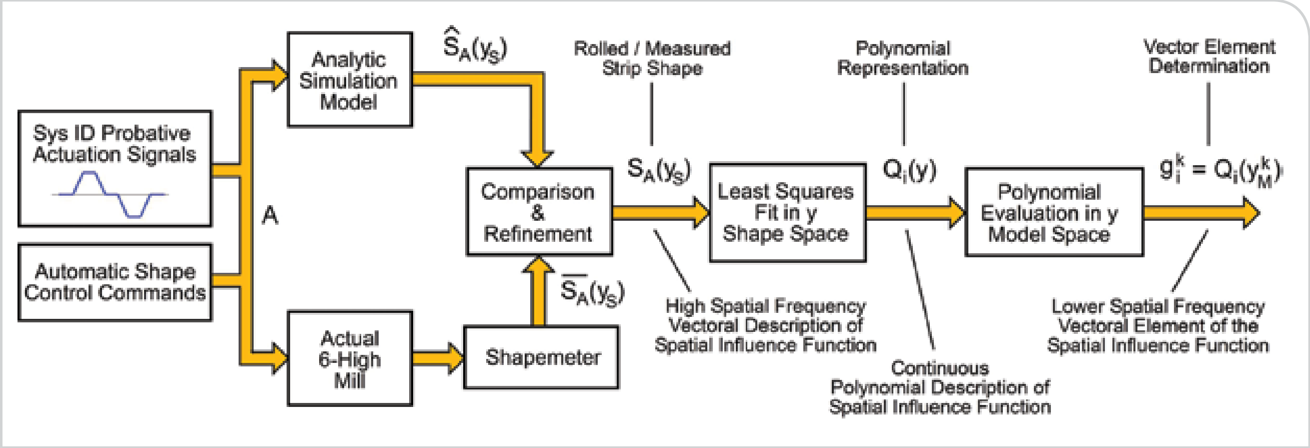

Block diagram showing the process of parameter identification of the G_M matrix (spatial influence functions).

Sobolev space) in monotonically increasing orders. The resulting coefficients, $\$_S^i$, provide a distribution/spectrum of spatial curvatures ingrained in the transverse stress waveform pattern (this is a type of parameterization). This type of distribution is akin to transformed descriptors like frequency responses and bode diagrams, and their relationships to a time response. The vector collection, $\$_S$, of the coefficients of Equation 8, provides a means of consolidating the parameterization of the describing spatial curvatures (forming a distribution/spectrum of curvature contributions).

$$\$_S = \left[\$_S^1 \quad \$_S^2 \quad \cdots \quad \$_S^{N_P} \right]^T$$

(Eq. 9)

Spatial Waveform Coordinate Frame — The orthogonal polynomials form a coordinate system in the directions of $\mathbf{P}_i(y)$. The transverse spatial waveform of a stress pattern, $\mathbf{S}(y)$, is represented in the $\mathbf{P}(y)$ coordinate system by a unique point or vector, $\$_S$, containing the spectra of curvatures forming $\mathbf{S}(y)$. If only the second- and fourth-order orthogonal polynomials are considered, it is possible to visualize the nature of the relationship between $\mathbf{S}(y)$ and $\$_S$ in terms of a Cartesian space/coordinate system.

Here, the location of a point within the Cartesian space (i.e., its vectoral coordinates) corresponds to the amplitudes of the spatial curvatures that, when combined, uniquely form the transverse spatial waveform pattern (akin to determining the time response of a pole within the Laplacian phase plane). Each point in this Cartesian space, $\$_S$, has a different corresponding transverse spatial waveform pattern. Likewise, through the linearity of the transformation, each transverse spatial waveform pattern will be represented by a unique point in the coordinate frame.

Figure 7 provides a "tour" of the waveform response characteristics (and associated strip shapes) for locations within the coordinate system.

Parametric Decomposition Using Orthogonal Polynomials — The Gram polynomials form an orthogonal basis, which implies the coefficients $\$_S^i$ can be determined through inner product methods, such that simple linear algebra can be used to perform this transformation. Over the discrete spatial sampling of y_M, and the inner product nature of Equation 8, a matrix transformation relationship is formed[3] from orthogonal polynomials evaluations:

$$\mathbf{S} = \tilde{\mathbf{P}}\$_S \quad \Leftrightarrow \quad \$_S = \left(\tilde{\mathbf{P}}^T\tilde{\mathbf{P}}\right)^{-1}\tilde{\mathbf{P}}^T\mathbf{S} = \tilde{\mathbf{P}}^T\mathbf{S} \quad \Leftrightarrow \quad \tilde{\mathbf{P}}^T\tilde{\mathbf{P}} = \mathbf{I}_{Np}$$

(Eq. 10)

where the matrix $\tilde{\mathbf{P}}$ is the curvature decomposition transform matrix,[3] and because of the polynomial orthogonality, the inverse transform matrix is its transpose.

Spatial Curvature Characteristics of the Rolled/Exit Shape — The spatial curvature distribution/spectrum of the rolled/exit shape is based on the waveform decomposition of the central relationships of Equations 1 and 6.[3]

$$\$_T \subseteq \$_S = \$_0 + \$_R + \$_A$$

(Eq. 11a)

$$= \$_0 + \$_R + \tilde{\mathbf{P}}^T\mathbf{G}_M\mathbf{A}$$

(Eq. 11b)

where

$\$_S \triangleq$ Rolled/exit strip shape's spatial curvature distribution/spectrum vector.

Figure 7

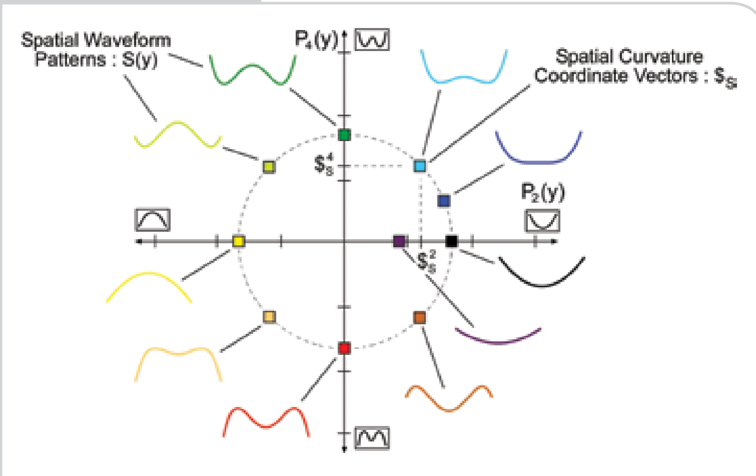

Diagram showing the nature of a transverse spatial waveform patterns and the location of their corresponding spatial curvature spectrum coordinate.

- $\$_T$ $\triangleq$ Shape target's spatial curvature distribution/spectrum vector, indicating the desired curvatures.
- $\$_0$ $\triangleq$ Incoming strip shape's spatial curvature distribution/spectrum vector.
- $\$_R$ $\triangleq$ Spatial curvature distribution/spectrum of the natural mechanical deformation characteristics of the roll stack and mill while under separating force loading. This component is static and cannot be modified during on-line/rolling operations.
- $\$_A$ $\triangleq$ Spatial curvature distribution/spectrum induced by the shape actuators.

Determination of Spatial Curvature Envelopes

The orthogonal polynomial-based coordinate framework of the section entitled "Spatial Waveform Coordinate Frame" provides a means of describing and coordinating the collection of spatial curvatures associated with a family of spatial waveform patterns. For a set/family of spatial waveform vectors, {S}, through the parameter decomposition of $\tilde{\mathbf{P}}^T$, a corresponding set of spatial curvature spectra, $\{\$_S\}$, exists:

$$\{\mathbf{S}\} \Rightarrow \tilde{\mathbf{P}}^T \Rightarrow \{\$_S\} \qquad \text{(Eq. 12)}$$

In the coordinate framework of "Spatial Waveform Coordinate Frame," the set $\{\$_S\}$ forms a grouping of points (an open set). These points populate a finite region, within this coordinate system framework, which can be over-contained by a closed surface/curve. This bounded, closed surface is the spatial curvature envelope for that specific set, $\{\$_S\}$.

Accommodating the Shape Actuation Constraints — The influences of the shape actuation systems are limited by the imposed operational and physical constraints, which define the set of constrained actuation vectors, $\bar{\mathbf{A}}$:

$$\bar{\mathbf{A}} = \{\mathbf{A}|_{\text{Constrained}}\} \qquad \text{(Eq. 13)}$$

For this application, the following constraints/limits will be considered:

- Stroke Limit — To comply with the hydraulic cylinder's stroke and/or working range.
- Force Limit — To comply with the hydraulic cylinder's force capacity, which may be asymmetric due to differences in the piston's blind-end/rod-end area differences.
- Rate Limit — To comply with restrictions in shifting movements due to rolling speed–related transverse friction loading.

This set is a collection of the available actuation inputs that, when applied to the mill, form a set of shape adjustment waveforms associated with the spatial influence functions, $\mathbf{G}_M$, and the shape actuation constraints, $\bar{\mathbf{A}}$.

$$\{\mathbf{S}_{\bar{A}}(y_M)\} = \{\mathbf{S}_{\bar{A}}\} = \mathbf{G}_M\bar{\mathbf{A}} \qquad \text{(Eq. 14)}$$

The corresponding spatial curvature representation is given by:

$$\{\$_{\bar{A}}\} = \tilde{\mathbf{P}}^T\mathbf{G}_M\bar{\mathbf{A}} \qquad \text{(Eq. 15)}$$

This set of spatial curvatures is the SACE.[3,4] The shape actuation constraints place limits on the extent of shape targets that can be achieved.

$$\{\$_T^{\text{Reachable}}\} = \$_0 + \$_R + \tilde{\mathbf{P}}^T\mathbf{G}_M\bar{\mathbf{A}} \qquad \text{(Eq. 16)}$$

This equation is the overall governing relationship. It defines a region, $\tilde{\mathbf{P}}^T\mathbf{G}_M\bar{\mathbf{A}}$ (SACE), that is offset by the incoming shape and roll cluster deformation vectors, $\$_0$ and $\$_R$, respectively. This *Offset* SACE is the set of achievable/reachable shape targets.[4]

Method of Determining the Bounding Spatial Curvature Envelope of the Constrained Shape Actuation — The basic process of determining the bounding SACE of $\$_{\bar{A}}$ involves the following steps:

1. Identify the set of all combinations of the constrained actuation, $\{\bar{\mathbf{A}}\}$, in terms of the constraints of the section entitled "Accommodating the Shape Actuation Constraints."
2. Apply an individual constrained actuation setting to the mill shape model component, $\mathbf{G}_M$, (based on the chosen conditions and operating point) to obtain the associated shape waveform, $\mathbf{S}_{\bar{A}}$.
3. Decompose the resulting shape waveform to its associated spatial curvature spectrum vector, $\$_{\bar{A}}$ (or evaluation of Equation 15).
4. Map the resulting spectral data (vector) within the curvature coordinate framework of "Spatial Waveform Coordinate Frame" (i.e., a point is plotted for each actuator setting).

These steps provide the ability to plot a single point, for each instance of the actuator settings, within the coordinate framework. As the actuator settings are varied over their entire constrained range, $\{\bar{\mathbf{A}}\}$, a collection of points develops, $\{\$_{\bar{A}}\}$.

The linear algebraic nature of the model, $\mathbf{G}_M$, and parameter decomposition of Equation 15 provide a convenient method of performing an exhaustive survey of the family of actuator settings, with relatively low computational effort. The grouping of points maps out/fills in a finite region of the curvature space (an open set). This region can be bounded by an over-containing, closed surface/curve that forms the spatial curvature envelope for the set $\{\$_{\bar{A}}\}$. This is the SACE for that specific condition/operating point. Figure 8 provides a flow chart and illustration of this process.

The nature of the closed surface/curve of the spatial curvature envelope is evaluated using multidimensional edge/extremity locating image processing techniques.[10] The determined extremities are interconnected by a multivariate interpolation method[13] that ensures a complete over-containment of the region's plotted points.

It is possible to simplify this approach by projecting the mapped points to a lower dimensional surface (e.g., the second-/fourth-order plane). This strategy provides a more practical (understandable) depiction of the envelope, but when evaluating the results, one must be cognizant of the influence of the "unseen" higher-dimensional content.

Development and Analysis of the SACEs

Using the parametric decomposition method, the SACEs are developed by examining only the shape actuation component of Equation 15 (i.e., $\$_A$). For a nominal roll stack setup (i.e., the selection of the individual roll diameter profiles/crowns), the shape actuators are preset to zero amplitudes. From this initial operating point, selected shape actuators are varied over their full scale ranges, and the resulting shape waveforms are collected/measured. The shape waveforms are transformed/decomposed into their associated distributions of spatial curvatures (curvature vectors/points), which are mapped within the curvature coordinate system.

Static Conditions — As noted in Table 1, the shape actuators have both static and dynamic components of their characteristic behavior/actions. The SACEs of the static settings describe the fullest extents of shape adjustment and are used in the selection of the mill setups and the presets of the shape actuators (potentially on a pass-by-pass basis).

SACE for Work Roll Crown and Bending: The most basic SACE is associated with variations in the work roll diameter crown and work roll bending, while all other conditions/settings are held constant. Figure 9a provides a plot showing the development of this SACE, the fundamental components and the orientations/ranges of their variability. It is interesting to note that increasing work roll crown induces a slightly stronger second-order response, while varying work roll bending has a stronger reaction in the fourth-order curvature, which is related to the familiar quarter buckle shape distortion. The resulting SACE is strongly oriented to the second-order curvature (note the scaling differences between the vertical and horizontal axes), with a dominance toward inducing tight edges and center buckle. The off-center nature of the nominal operating point (origin) within the SACE is associated with asymmetric roll bending forces related to the blind-end/rod-end differentials of the actuating hydraulic cylinders.

SACE for Backup Roll Crown: Figure 9b shows the reaction of the SACE to changes in the backup roll diameter crown. As expected, the SACE is migrated toward a more positive second-order crown-in condition, but it is also rotated clockwise and slightly "squashed" in the fourth-order response. This rotation effect is associated with the addition of a dominant

Figure 8

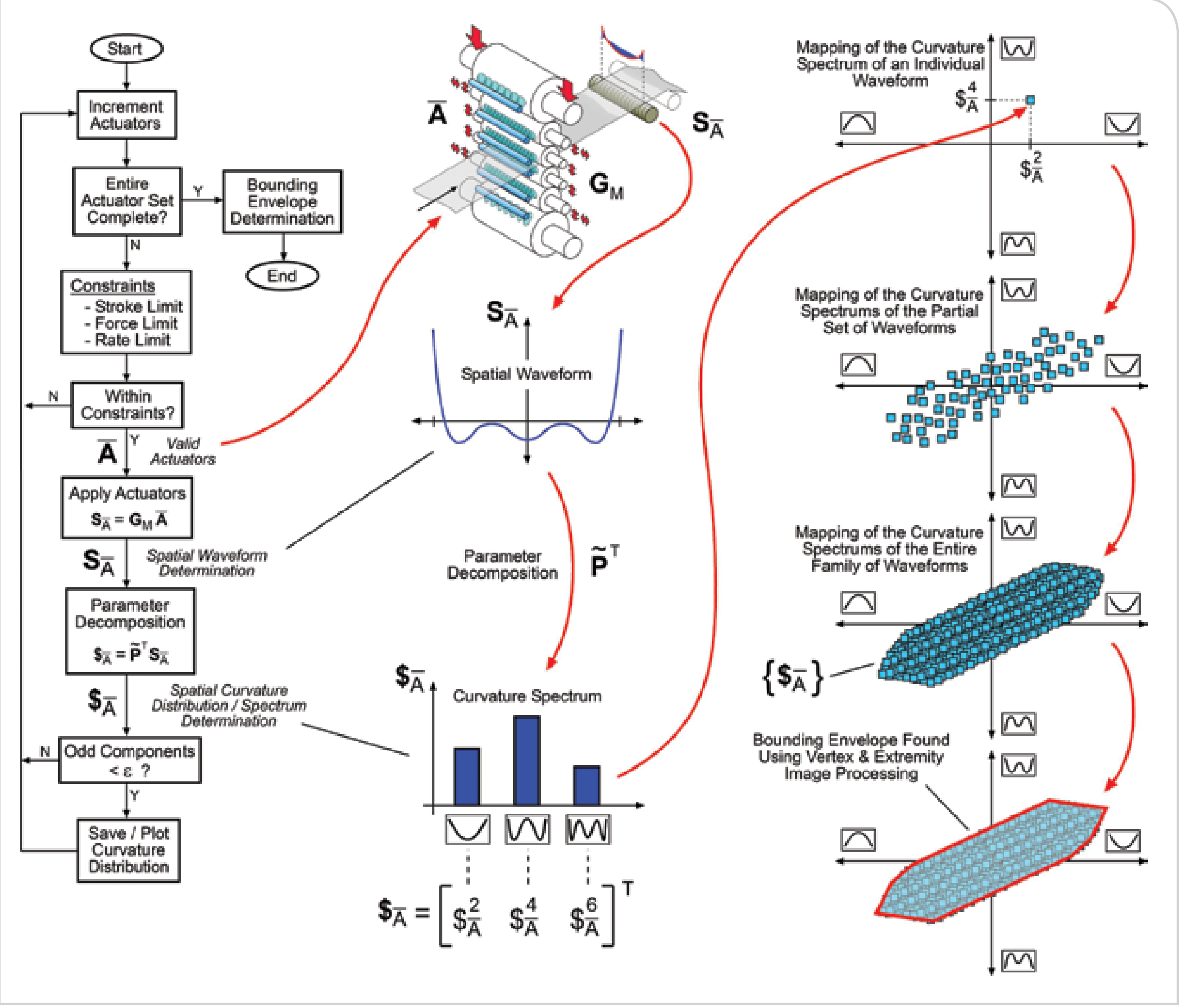

Process of determining the bounding spatial curvature envelope (SACE) associated with the family of transverse shape waveforms generated by the full range of the constrained shape actuation.

mechanical crown within the roll stack, which suppresses certain fourth-order components. Tapering the backup roll provides similar results and can be adjusted to more directly address strip edge conditions.

SACE for Changes in Strip Width: From a nominal operating point, and changing no other parameters/conditions, a reduction in the strip width induces a corresponding reduction in the sensitivities and ranges of the shape actuators' influence. As shown in Figure 10a, the resulting SACE "shrinks" as the strip width is reduced (with all other conditions/settings held constant). As might be expected, it also migrates toward loose edges in both the second- and fourth-order curvatures. For certain mill configurations and setups, a slight clockwise rotation has also been noted. This is believed to stem from the crown effects of the other rolls within the stack, where certain crown configurations may induce a center region flattening (on narrow strip for all work roll bending settings). This flattening waveform is created by the added fourth-order curvature provided by the rotation. These results correlate with the observations noted on 20-high cluster mills.[4]

SACE for Changes in Strip Thickness: As the strip thickness is reduced, the strip's aspect ratio (width/thickness) increases. As the aspect ratio increases, the strip's ability to store transverse shape distortions is diminished (i.e., the thinner strip tends to expose its stress patterns more efficiently). As shown in

Figure 9

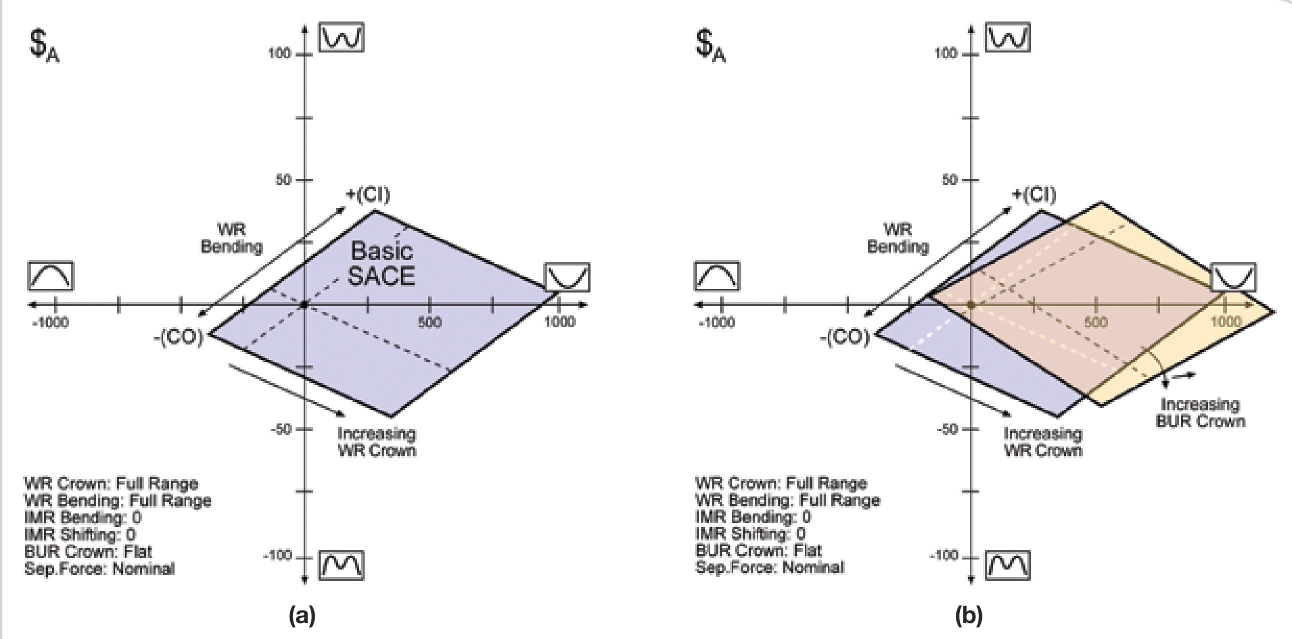

Plots showing the development of the basic SACEs associated with work roll crown and work roll bending (a), and the variation due to an increase in the backup roll crown (b).

Figure 10b, this results in a greater shape actuator sensitivity (larger SACE) as the strip thickness is reduced. These results are well correlated to the observations noted on 20-high cluster mills.[4] It is important to note the correlation between the strip thickness reaction and the strip width reaction shown in Figure 10a. The similarity of responses is associated with the resulting aspect ratios (wider/thinner have similar stress storage behaviors, likewise to narrow/thicker).

SACE for Changes in Yield Stress: As pass-to-pass reductions reduce the strip thickness, the material is work hardened (increasing the yield stress). As shown in Figure 10c, the SACE does not expand, but only rotates as the strip yield stress increases. This is associated with a degree of the strip's increased resistance to shape adjustment, and also due to an increased level of fourth-order involvement associated with a suppression of roll stack deformations in the center of the strip. These results correlate with observations noted on 20-high cluster mills.[4]

SACE for Intermediate Roll Bending: The basic SACE (Figure 9, work roll crown and bending) can be extended by the application of intermediate roll (IMR) bending (Figure 11a). It is interesting to note that the IMR bending function is not oriented in the same direction as the work roll bending. IMR bending induces a stronger second-order response that is more closely related to work roll crowning actions. This is due to the attenuation of the IMR bending (to the roll bite) by the work roll's resistance to deformation. The resulting SACE is "stretched" strongly along the second-order curvature (note the scaling differences between the vertical and horizontal axes), with a dominance toward inducing tight edges and center buckle.

SACE for Intermediate Roll Shifting: The expanded SACE (Figure 11a, work roll crown, bending and IMR bending) can be further extended by the application of IMR shifting (assuming complex crowns), as shown in Figure 11b. It is interesting to note that the IMR shifting function is very similar to work roll crowning actions (with a slightly shallower slope), and due to its bipolar capabilities, has an extended dynamic range. The resulting SACE is "stretched" strongly and broadly along the second-order curvature. The shallower IMR shifting function induces a more exaggerated level of tight edges and center buckle.

Dynamic Conditions — During active rolling operations, where on-line shape control activities are in effect, the dynamic response characteristics of the shape actuators must be considered in the control decisions and performance expectations.

As noted in Table 1, the fast-acting shape actuators are the work roll and IMR bending. The speed of response of these hydraulic actuators is not a function of the rolling speed or other conditions, and is therefore always available and fast. Figure 12 provides a pair

Figure 10

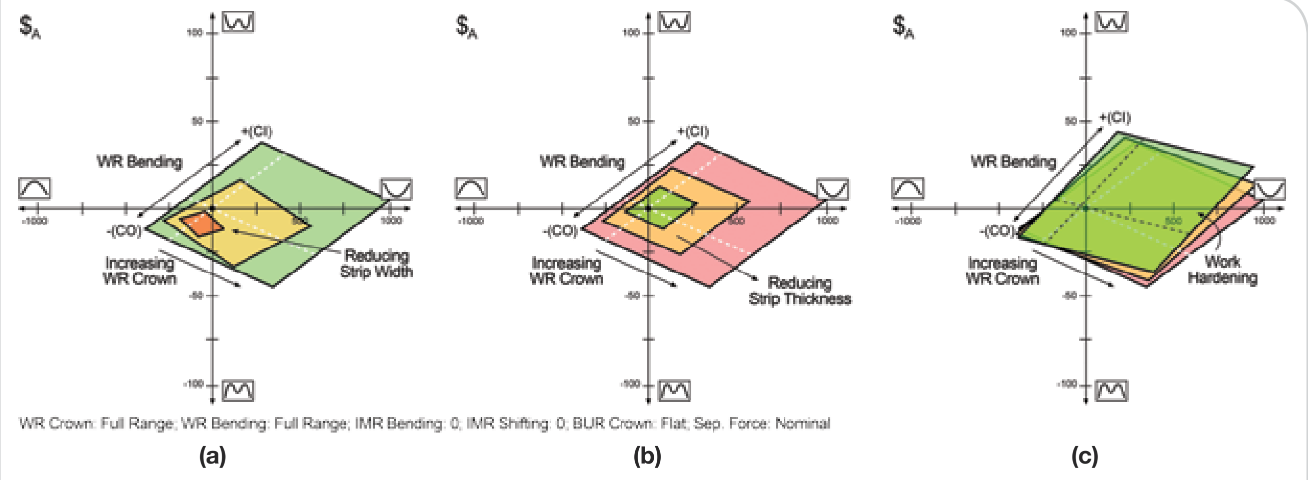

Plots showing the SACEs associated with changes in strip width (a), thickness (b) and yield stress (c).

of plots showing the development of the fast-acting SACE (*Fast* SACE). It is important to note that the *Fast* SACE has a rather compressed overall size (it is only a function of the work roll and IMR bending). The *Fast* SACE directly indicates the extent of rapid shape corrections that can be provided, which means that care must be taken in the selection of the initial conditions, since the transient convergence to the shape target must be reachable by these actuators.

If the shape correction adjustments exceed the extent of the *Fast* SACE, then it will be necessary to involve the slower-acting shape actuators (IMR shifting and zonal coolant) to expand the SACE (or translate the *Fast* SACE). Figure 12b shows the relative expansion of the SACE associated with IMR shifting. This expanded SACE provides a significant enhancement of the shape actuation capabilities, but the speed restrictions of the IMR shifting may cause an undesirable reduction in the rolled strip shape

Figure 11

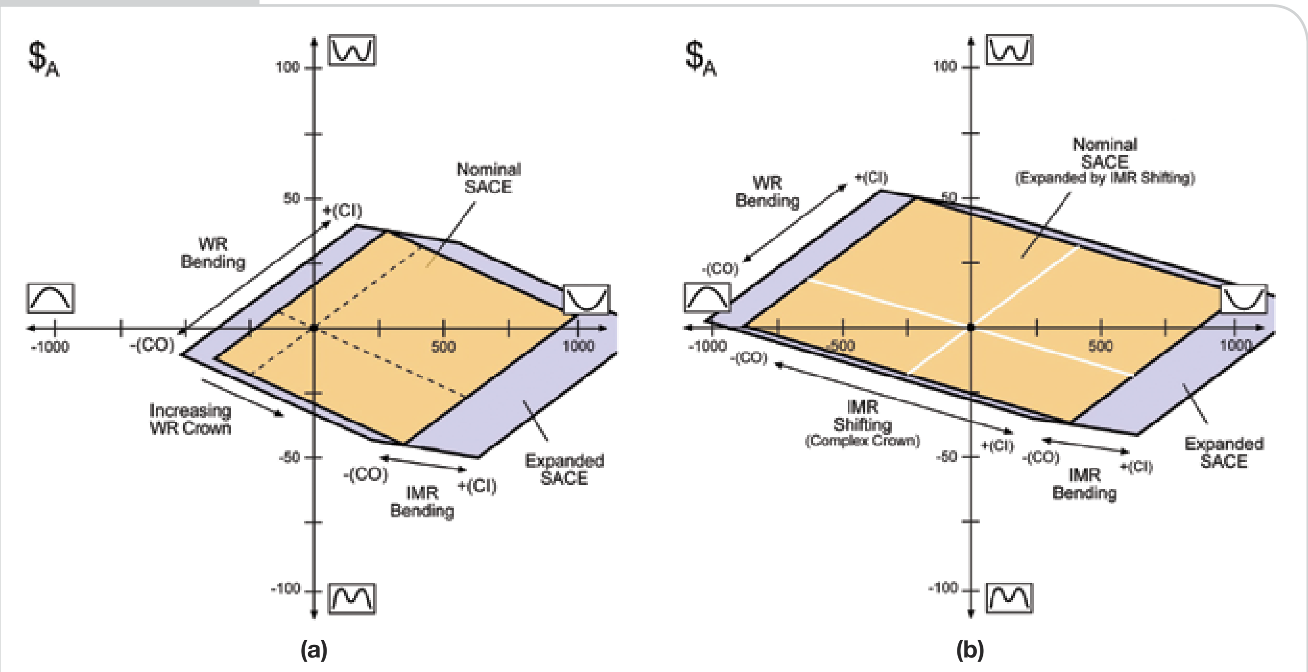

Plots showing the expansion of the SACE associated with intermediate roll bending and shifting.

control quality (while waiting for the slow-acting IMR shifting to take effect).

In a sense, the slow-acting IMR shifting actuation, $\$_R^{IS}$, can be considered as a setup of the static roll stack deflection term, $\$_R$, which induces a translation of the *Fast* SACE in the direction of IMR shifting. From a rolling operations and mill setup design perspective, the pseudo-static/dynamic term ($\$_R^{IS}$) can be used as a surrogate to modifications in the work roll crown. As shown in Figure 12, this term operates along the direction of the IMR shifting action.

Shape Target Reachability and Directions of Actuation Improvement

As developed in Reference 4 and considering Equations 7 and 16, for an arbitrary pass k, the shape target spatial curvatures, $\$_T|_k$, must reside within the *Offset* SACE.

$$\$_T\Big|_k \subseteq \left\{\$_T^{\text{Reachable}}\right\}\Big|_k = \overbrace{\overbrace{\$_0\Big|_k + \$_R\Big|_k}^{\textit{Offset}\text{ Vector}} + \overbrace{\tilde{\mathbf{P}}^T\,\mathbf{G}_M\Big|_k\,\bar{\mathbf{A}}\Big|_k}^{\text{SACE}}}^{\textit{Offset}\text{ SACE}}$$

$$\text{for } k = 1, 2, 3, \ldots \text{(includes payoff/loading pass)} \qquad \text{(Eq. 17)}$$

For a given pass, the *Offset* SACE is determined by the vectoral summation of the incoming strip shape and roll cluster deformation spatial curvatures, $\$_0|_k$ and $\$_R|_k$, respectively, to form an offset vector. The origin of the SACE ($\tilde{\mathbf{P}}^T\mathbf{G}_M|_k\bar{\mathbf{A}}|_k$) is then displaced by the offset vector. For a multipass coil to be successfully rolled, this relationship must be satisfied on a pass-to-pass basis (or, at the very least, on the final pass). This involves coordinating the pass-to-pass progressions of the shape target, pass scheduled roll stack deformation and available range of shape actuation.

Assessing whether a given pass' shape target is reachable reduces to determining if the shape target resides within the bounds of the *Offset* SACE. In a vertical stack configuration, the fast-acting shape actuation (i.e., *Offset Fast* SACE) is critical, since the actuators of this region will be able to address the dynamic aspects of the pass' profile (primarily acceleration/deceleration) and can immediately address incoming shape disturbances (see text in red in Table 1).

In considering the *Offset Fast* SACE, the pass-to-pass contribution of the slow-acting IMR shifting, $\$_R^{IS}|_k$, is seen as an added offset component (but not exactly in the static sense). Although a dynamic shape actuator, the slow response of IMR shifting is more akin to an adjustable component of the static roll stack deflection, $\$_R|_k$. Here it is useful to design the pass scheduled separating force profile and roll stack setup to require a constant preset of $\$_R^{IS}$, which would

Figure 12

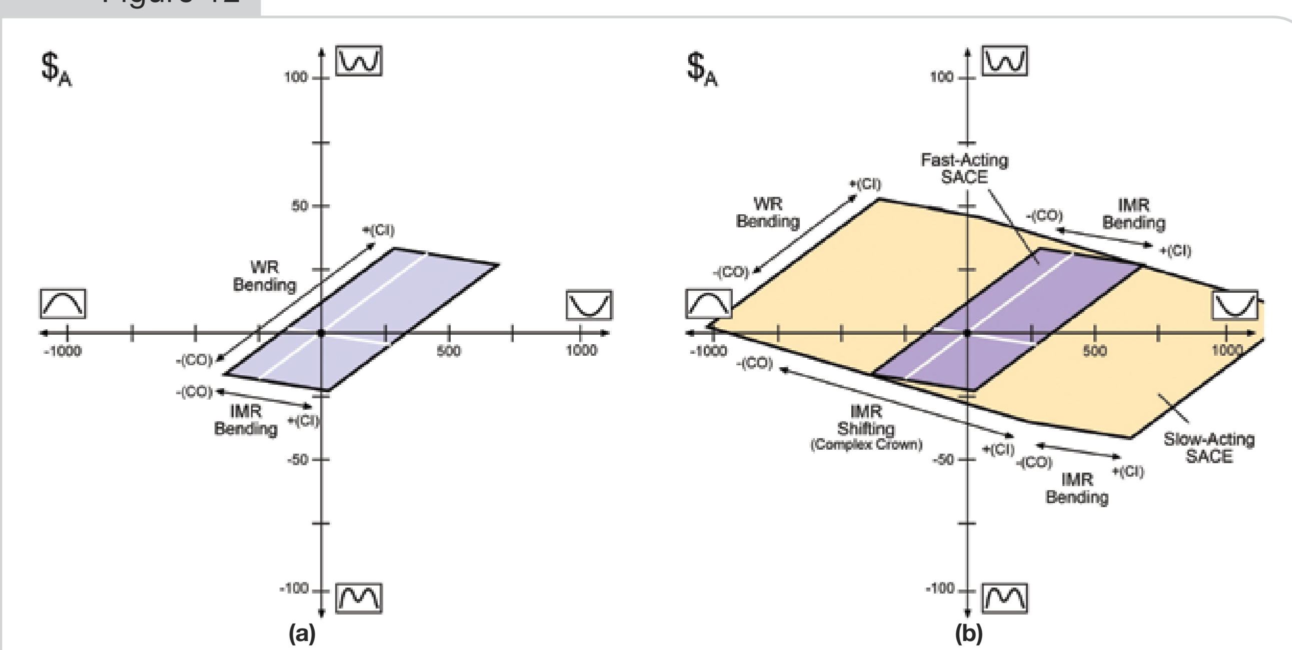

Plots showing the condensed SACE control range available from the fast-acting dynamic shape adjustment (a) and the slower (b) but expanded SACE-associated IMR shifting.

be applied prior to closing the gap to initiate the first pass. If this is not practical, then it is desirable to design the pass schedule in such a way as to minimize the pass-to-pass deviation in $\$_R^{IS}|_k$ such that the transient effects of the shifting motion are completed early in the pass. Alternatively, the IMR shifting component (for all passes) can also be accommodated by the selection of the work roll mechanical crown.

Figure 13 shows the entire pass-to-pass progression of the *Offset* SACE and *Offset Fast* SACE, along with the sequence of desired shape targets and pass scheduled roll stack deflections. As noted in Figure 13, with a nominal IMR shifting preset, the shape targets of passes 1, 2, 3 and 7 are not over-contained by the *Offset Fast* SACE, and therefore are not reachable by the constrained actuation without an IMR shifting action. Also shown in Figure 13, if pass 1 is excluded, by applying a preset IMR shift (in the direction of more roll stack crown than nominal), the *Offset Fast* SACE over-contains the shape target on all remaining passes. The highlighted details of passes 6 and 7 illustrate how the *Offset Fast* SACE is translated to accommodate the shape targets.

Conclusion

This paper has examined the nature and extent of the shape actuation capabilities of 6-high cold mills (with 4-high configurations being of reduced order through the elimination of IMR bending and shifting). The method used employs an adaptive matrix model (formed from measured and modeled results) and a computationally efficient linear algebraic parameter

Figure 13

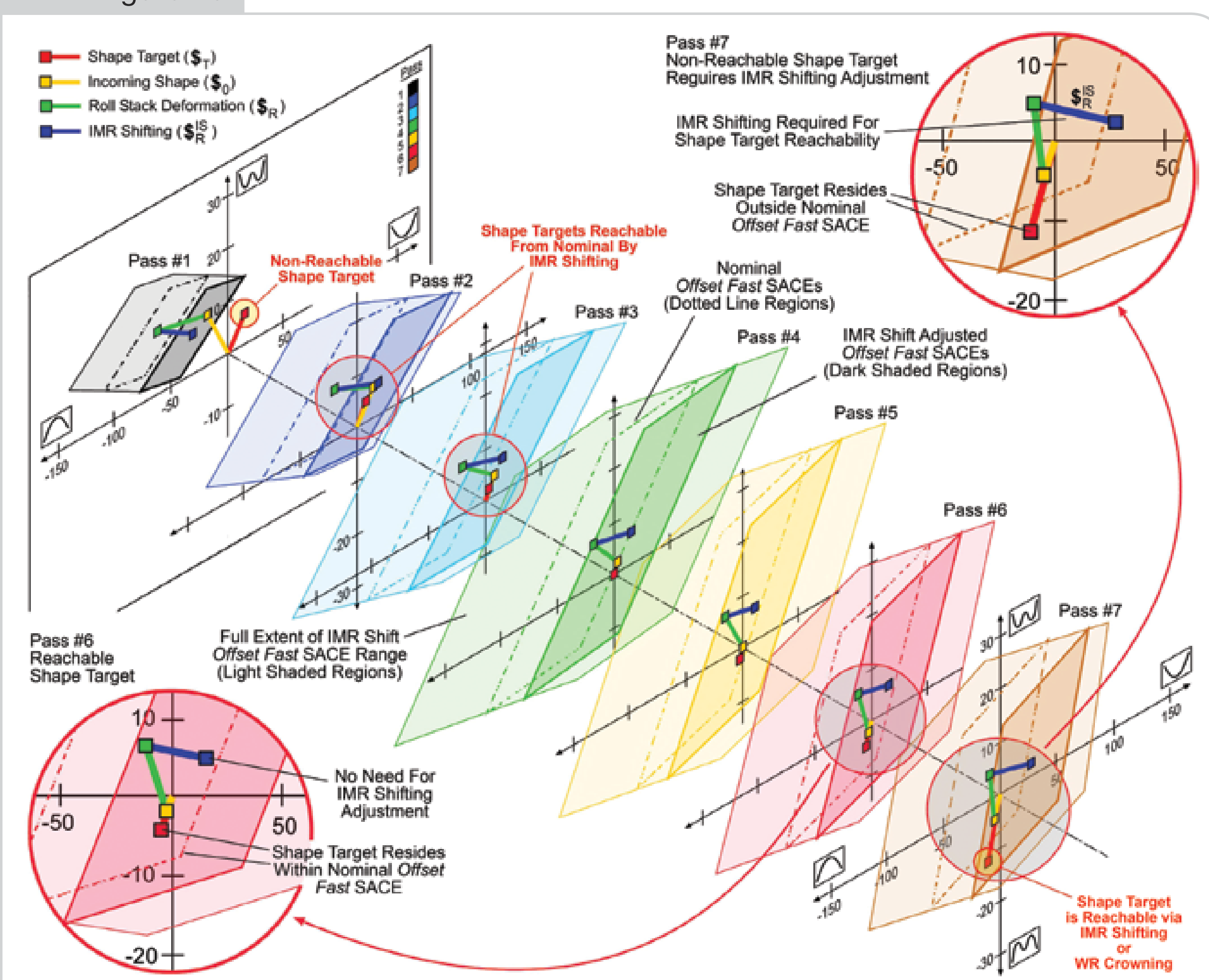

Pass-to-pass progression showing the relationships of the *Offset* SACEs, the nominal *Offset Fast* SACEs and the shape targets, along with the corrective actions of IMR shifting and associated translations of the *Offset Fast* SACEs.

decomposition transformation to characterize the range of spatial curvatures that can be induced by the shape actuation systems, in an orthogonal polynomial coordinate system. The extent of the shape actuation influence for a given operating condition is described by the shape actuation capabilities envelope (SACE), which is formed in a shape/stress framework that is amenable to direct measurement by shapemeters.

This provides an alternate approach to classical control range analysis methods based on roll gap profile modeling. The nature of the resulting SACEs are directly correlated to the control range descriptions, because they are both characterizing the same phenomena. Because this approach is formed in a shape/stress framework, it provides much-needed insight/guidance into how the pass schedule, shape targets, roll stack setup (roll stack diameter profiles, complex crown/taper selections, etc.) and shape actuator presets can be modified to achieve the shape target reachability criteria for either a specific condition or over a pass-to-pass sequence.

The key aspects of this method are as follows:

- Based on a consistent analytic framework that is abstracted from and independent of the mill configuration and arrangement.
- Arbitrary transverse spatial resolution (fine enough to accommodate zonal coolant sprays).
- The orthogonal polynomial representations provide spatial curvature descriptions and an inherent vector space basis set (coordinate system).
- Fully scalable odd and even orders of curvature (up to and beyond the 60th order).
- Computationally efficient analytic framework.
- Applicable to asymmetric transverse strip thickness profiles (wedged strip).

And perhaps most importantly:

- The orthogonal polynomial coordinate system is scaled in shape/stress units and is therefore directly applicable to shape target reachability studies.[4]
- The results can be directly measured and validated by on-line shapemeter readings.

This work is a segment of continuing research into developing a set of analytic, operational tools to support and give insight into:

- Selecting mechanical crown and mill setup.
- Predicting shape actuation performance and capabilities.
- Determining reachable shape targets.
- Coordinating pass scheduling and shape target progression.
- Identifying the range of incoming shape distortions that can be accommodated.
- Assisting in the resolution of complex shape/flatness problems.

References

1. Hata, K., et al., "Universal Crown Control Mills," *Hitachi Review,* Vol. 34, No. 4, 1985, pp. 168–174.
2. Ginzburg, V.B., *Fundamentals of Flat Rolling,* Marcel Dekker Inc., New York, N.Y., 2000, pp. 819–820.
3. Zipf, M.E., "Method for the Determination of Shape Actuator Capabilities Envelopes in 20-High Cluster Mills," *Iron & Steel Technology,* Vol. 9, No. 12, 2012, pp. 77–89.
4. Zipf, M.E., "Multivariable Directions in the Improvement of Shape Actuator Performance," *Iron & Steel Technology,* Vol. 10, No. 2, 2013, pp. 106–123.
5. Zipf, M.E., "20-High Cluster Mill Shape Actuator Characterization Through Parameter Identification Methods," *Proceedings of the Associação Brasileira de Metalurgia e Materiais, 47th Rolling Seminar — Processes, Rolled and Coated Products,* 26–29 October 2010, Belo Horizonte, MG, Brazil.
6. Grimble, M.J., and Fotakis, J., "The Design of Strip Shape Control Systems for Sendzimir Mills," *IEEE Transactions on Automatic Control,* Vol. AC-27, No. 3, June 1982, pp. 656–666.
7. Ringwood, J.V., and Grimble, M.J., "Shape Control in Sendzimir Mills Using Both Crown and Intermediate Roll Actuators," *IEEE Transactions on Automatic Control,* Vol. 35, No. 4, April 1990, pp. 453–459.
8. Ringwood, J.V., "Shape Control Systems for Sendzimir Steel Mills," *IEEE Transactions on Control System Technology,* Vol. 8, No. 1, January 2000, pp. 70–86.
9. Timan, A.F., *Theory of Approximation of Functions of a Real Variable,* Dover Publications Inc., Mineola, N.Y., 1963.
10. Hall, E.L., *Computer Image Processing and Recognition,* Academic Press, New York, N.Y., 1979, pp. 390–412.
11. Guo, R.M., "Development of Bi-Directional Two-Stage Transport Matrix Method for Strip Profile and Shape Calculation," *Proceedings of the 4th International Conference on Modeling and Simulation of Metallurgical Processes in Steelmaking (STEELSIM), METEC,* Düsseldorf, Germany, 27 June–1 July 2011.
12. Stone, M.D., and Gray, R., "Theory and Practical Aspects in Crown Control," *Iron and Steel Engineer Year Book,* 1965, pp. 657–667.
13. Press, W.H.; Flannery, B.P.; Teukolsky, S.A.; and Vetterling, W.T., *Numerical Recipes: The Art of Scientific Computing,* Cambridge University Press, New York, N.Y., 1986. ✦

This paper was presented at AISTech 2013 — The Iron & Steel Technology Conference and Exposition, Pittsburgh, Pa., and published in the Conference Proceedings.